JOURNAL OF COMPUTATIONAL PHYSICS **142,** 129–147 (1998)
ARTICLE NO. CP985938

On the Analysis and Construction of Perfectly Matched Layers for the Linearized Euler Equations

J. S. Hesthaven

Division of Applied Mathematics, Brown University, Box F, Providence, Rhode Island 02912
E-mail: jansh@cfm.brown.edu

Received July l0, 1997; revised January 29, 1998

We present a detailed analysis of a recently proposed perfectly matched layer (PML) method for the absorption of acoustic waves. The split set of equations is shown to be only weakly well-posed, and ill-posed under small low order perturbations. This analysis provides the explanation for the stability problems associated with the spilt field formulation and illustrates why applying a filter has a stabilizing effect. Utilizing recent results obtained within the context of electromagnetics, we develop strongly well-posed absorbing layers for the linearized Euler equations. The schemes are shown to be perfectly absorbing independent of frequency and angle of incidence of the wave in the case of a non-convecting mean flow. In the general case of a convecting mean flow, a number of techniques is combined to obtain absorbing layers exhibiting PML-like behavior. The efficacy of the absorbing layers is illustrated though the solution of aero-acoustic benchmark problems.

1. INTRODUCTION

When solving wave-dominated problems, as they appear in aero-acoustics or electromagnetics, one often encounters the problem of how to accurately obtain infinite domain solutions using a finite computational domain. The truncation of the computational domain must be done in a way that avoids, at least approximately, the excitation of reflected waves which might otherwise contaminate the computational domain and falsify the solution.

The issue of how to properly devise such boundary conditions at an artificial computational boundary has received much attention in past. The use of characteristic boundary conditions [1] is appealing due to its simplicity, but is only accurate for close to perpendicular incidence of the wave. More elaborate schemes involve radiation boundary conditions based on localization of the Dirichlet-to-Neumann map [2, 3] or an asymptotic expansion of the far-field solution [4]. A fairly recent review of there methods can be found in [5].

0021-9991/98 $25.00

Alternatives to such schemes involve the introduction of buffer or sponge layers in which the waves are either damped [6], accelerated to supersonic conditions [7], decelerated [8], or attenuated by combinations thereof [9]. The construction of these latter schemes are in most cases based on physical arguments with little theoretical evidence of their, often quite remarkable, performance.

In the context of electromagnetics, Berenger [10] recently proposed a novel way by which to derive the sought after absorbing boundary conditions. By splitting Maxwells equations in an unphysical manner, additional degrees of freedom are introduced. This allows for the construction of non-reflecting absorbing layers with the remarkable property that they maintain their absorbing properties irrespective of the frequency and angle of propagation of the incident wave, i.e., this approach appears to provide an optimal absorbing boundary condition and have spawned a hectic research into such layers, termed Perfectly Matched Layers (PML). While the PML scheme has been applied successfully during the last years, it was recently proven [11] that the particular splitting of Maxwells equations employed in [10] renders the resulting set of equations weakly well-posed and ill-posed under arbitrary low order perturbations, i.e., numerical solution of these equations can be expected to be unconditionally unstable, an example of such being provided in [11]. This realization has focused the attention towards alternative well-posed formulations of the electromagnetic PML methods and several such schemes have been proposed in recent years, see for instance [12–16]. Hence, although the original PML schemes have proven erroneous, the general approach has proven extremely fruitful and has allowed for the computation of problems in electromagnetics of unsurpassed accuracy.

Inspired by the success of the PML methods for Maxwells equations, Hu [17] recently proposed a PML method for the equations of acoustics by taking an approach very similar to the one originally developed for Maxwells equations, i.e., by splitting the equations of acoustics in an unphysical manner. Although the general approach is the same as in [10], the details of the split-field formulation is different, hence leading to a different PML scheme with different properties. Indeed, contrary to most work within the community of electromagnetics, Hu [17] reported the need for using a low pass filter inside the absorbing layers to maintain stability of the scheme. A similar observation was made in [18] where no filter was applied and the numerical solutions are found to exhibit exponential growth. This points to an inherent instability of the scheme and in [18] a partial explanation, in terms of loss of strong well-posedness in certain special cases, is provided.

In the present work we provide a complete analysis of the split PML scheme of [17], confirming the speculations put forward in [18] in a more general context. Indeed, the scheme of [17] is found to be only weakly well-posed in the two-dimensional case and ill-posed under low order perturbations, although the details of the nature of the instability is different from that discussed in [11]. We proceed by presenting a well-posed PML scheme for the non-convective equations of acoustics and, for the more general convective case, a well-posed absorbing layer exhibiting PML-like behavior.

The remainder of this paper is organized as follows. In Section 2 we introduce the equations of acoustics as obtained from the linearized Euler equations. Section 3 contains the first part of the paper in which we present an analysis of the PML method recently proposed in [17] and we provide an explanation for the problems of maintaining stability as reported in [17, 18]. This leads to Section 4 where we present an alternative to the unstable PML scheme. For the case of a non-convection mean flow we construct a well behaved PML method and illustrate its performance through numerical experiments. For the general

case of a convective mean flow, we propose to apply a combination of techniques to arrive at absorbing layers with PML-like behavior and support the reasoning by numerical studies. Section 5 contains a few concluding remarks.

2. THE EQUATIONS OF ACOUSTICS

We shall consider the two-dimensional, linearized, compressible Euler equations on the form

$$\frac{\partial \boldsymbol{q}}{\partial t} + A\frac{\partial \boldsymbol{q}}{\partial x} + B\frac{\partial \boldsymbol{q}}{\partial y} = 0, \tag{1}$$

where the state vector, $\boldsymbol{q}$, and the constant matrices, A and B, are given as

$$\boldsymbol{q} = \begin{bmatrix} \rho \\ u \\ v \\ p \end{bmatrix}, \qquad A = \begin{bmatrix} M & 1 & 0 & 0 \\ 0 & M & 0 & 1 \\ 0 & 0 & M & 0 \\ 0 & 1 & 0 & M \end{bmatrix}, \qquad B = \begin{bmatrix} 0 & 0 & 1 & 0 \\ 0 & 0 & 0 & 0 \\ 0 & 0 & 0 & 1 \\ 0 & 0 & 1 & 0 \end{bmatrix}. \tag{2}$$

These equations are recovered from the Euler equations by linearizing around the uniform mean state, $(\rho_0, u_0, 0, p_0)$, and introducing the normalization

$$t = \frac{tc_0}{L}, \qquad x = \frac{x}{L}, \qquad y = \frac{y}{L}, \qquad \boldsymbol{q} = \left[\frac{\rho}{\rho_0}, \frac{u}{c_0}, \frac{v}{c_0}, \frac{p}{\rho_0 c_0^2}\right]^T,$$

where L represents a characteristic length while $c_0 = \sqrt{\gamma p_0/\rho_0}$ refers to the sound speed of the mean flow. In this context, Eqs. (1)–(2), describe the propagation and interaction of waves in a parallel uniform flow with a Mach number, $M = u_0/c_0$. Choosing $v_0 = 0$ does not introduce any restrictions on the analysis as the general situation may always be rotated to arrive at this particular case.

A deeper understanding of the underlying properties, physical as well as mathematical, of Eqs. (1)–(2) can be gained by introducing the similarity transform

$$S = \frac{1}{2}\begin{bmatrix} 1 & 2 & 0 & 1 \\ 1 & 0 & 0 & -1 \\ 0 & 0 & 2 & 0 \\ 1 & 0 & 0 & 1 \end{bmatrix}, \qquad S^{-1} = \begin{bmatrix} 0 & 1 & 0 & 1 \\ 1 & 0 & 0 & -1 \\ 0 & 0 & 1 & 0 \\ 0 & -1 & 0 & 1 \end{bmatrix},$$

to obtain

$$S^{-1}AS = \begin{bmatrix} M+1 & 0 & 0 & 0 \\ 0 & M & 0 & 0 \\ 0 & 0 & M & 0 \\ 0 & 0 & 0 & M-1 \end{bmatrix}, \qquad S^{-1}BS = \frac{1}{2}\begin{bmatrix} 0 & 0 & 2 & 0 \\ 0 & 0 & 0 & 0 \\ 1 & 0 & 0 & 1 \\ 0 & 0 & 2 & 0 \end{bmatrix},$$

where $S^{-1}\boldsymbol{q} = \boldsymbol{R} = [p+u, \rho - p, v, p-u]^T$ represents the characteristic variables. We recognize the two convective entropy (R_2) and vorticity waves (R_3), respectively, and the co- (R_1) and counter-propagating (R_4) sounds waves through which the complete physical scenario can be understood.

However, the similarity transformation also shows that A and B can be transformed such as to become symmetric simultaneously by multiplication with a positive definite diagonal matrix. This implies that Eqs. (1)–(2) form a strongly well-posed hyperbolic system [19] and

that the well-posedness of Eqs. (1)–(2) is unaffected by the addition of low order terms. As we shall see shortly, lack of strong well-posedness can have serious consequences and make the construction of convergent numerical schemes impossible due to inherent instabilities of the system of equations.

By inspecting Eqs. (1)–(2) it is clear that the equation for ρ plays a passive role only. Hence, for the sake of simplicity, and without loss of generality, we shall perform the subsequent analysis for the $[u, v, p]^T$ system only as the behavior of ρ can be inferred from p. However, the computational results are obtained for the full set of equations.

3. AN ANALYSIS OF THE SPLIT-FIELD PML METHOD

Following the line of thought initiated in [10] for the development of perfectly matched layers (PML) for electromagnetics, Hu [17] recently proposed a split-field PML scheme for the two-dimensional linearized Euler equations, Eqs. (1)–(2). Different from the approach of [10], in which only some of the field components are split, in [17] all the field components of $\boldsymbol{q}$ are split to arrive at a set of equations to be solved in the layer of the form

$$\frac{\partial \boldsymbol{q}^s}{\partial t} + A^s \frac{\partial \boldsymbol{q}^s}{\partial x} + B^s \frac{\partial \boldsymbol{q}^s}{\partial y} + C^s \boldsymbol{q}^s = 0, \tag{3}$$

where $\boldsymbol{q}^s = [u_1, u_2, v_1, v_2, p_1, p_2]^T$, such that $p = p_1 + p_2$ and likewise for the velocity components. The 6×6 matrices in Eq. (3) are given as [17]

$$A^s = \begin{bmatrix} 0 & 0 & 0 & 0 & 1 & 1 \\ M & M & 0 & 0 & 0 & 0 \\ 0 & 0 & 0 & 0 & 0 & 0 \\ 0 & 0 & M & M & 0 & 0 \\ 1 & 1 & 0 & 0 & M & M \\ 0 & 0 & 0 & 0 & 0 & 0 \end{bmatrix}, \qquad B^s = \begin{bmatrix} 0 & 0 & 0 & 0 & 0 & 0 \\ 0 & 0 & 0 & 0 & 0 & 0 \\ 0 & 0 & 0 & 0 & 1 & 1 \\ 0 & 0 & 0 & 0 & 0 & 0 \\ 0 & 0 & 0 & 0 & 0 & 0 \\ 0 & 0 & 1 & 1 & 0 & 0 \end{bmatrix}, \tag{4}$$

while $C^s = \mathrm{diag}(\sigma_x, \sigma_x, \sigma_y, \sigma_x, \sigma_x, \sigma_y)$ represents the diagonal matrix responsible for the dissipation of the waves. Note that we have reduced the system of equations as compared to [17] by removing the equation describing the behavior of the density, ρ. However, as discussed above this does restrict the generality of the subsequent analysis.

The use of split variables may, at first, seem perfectly legal since for $\sigma_x = \sigma_y = 0$ the original equations are recovered by adding the equations for the split fields. This reasoning, however, is faulty as we shall show in the following.

Let us first address the issue of well-posedness of the split system of equations, Eqs. (3)–(4), and recall that the question of well-posedness of the system is unaffected by the low order term, $C^s \boldsymbol{q}^s$, which we therefore neglect. We begin by considering the diagonalizing similarity transform of A^s given as

$$S = \begin{bmatrix} 0 & 0 & -1 & \frac{1}{M-1} & 0 & \frac{1}{M+1} \\ 0 & 0 & 1 & \frac{-M}{M-1} & 0 & \frac{M}{M+1} \\ 0 & -1 & 0 & 0 & 0 & 0 \\ 0 & 1 & 0 & 0 & 1 & 0 \\ -1 & 0 & 0 & 1 & 0 & 1 \\ 1 & 0 & 0 & 0 & 0 & 0 \end{bmatrix}, \qquad S^{-1} = \begin{bmatrix} 0 & 0 & 0 & 0 & 0 & 1 \\ 0 & 0 & 1 & 0 & 0 & 0 \\ \frac{-M^2}{M^2-1} & \frac{-1}{M^2-1} & 0 & 0 & \frac{M}{M^2-1} & \frac{M}{M^2-1} \\ -\frac{1}{2} & -\frac{1}{2} & 0 & 0 & \frac{1}{2} & \frac{1}{2} \\ 0 & 0 & 1 & 1 & 0 & 0 \\ \frac{1}{2} & \frac{1}{2} & 0 & 0 & \frac{1}{2} & \frac{1}{2} \end{bmatrix},$$

resulting in $S^{-1}A^sS = \mathrm{diag}(0, 0, 0, M-1, M, M+1)$, i.e., 3 zero eigenvalues have been introduced as a consequence of the splitting. It is straightforward to show that these three additional eigenvalues imply that S and S^{-1} cannot transform B^s into a matrix that can be made symmetric by multiplication with a positive definite diagonal matrix, i.e., A^s and B^s cannot be symmetrized simultaneously [20]. This observation, however, is not conclusive in terms of lack of strong well-posedness of Eqs. (3)–(4), but it remains a concern as the split set of equations has lost an important symmetry property as compared to Eqs. (1)–(2).

To continue the analysis we shall focus the attention on the Cauchy problem, i.e., neglect the effect of the boundary conditions in Eqs. (3)–(4). We introduce the spatial Fourier transform of $\boldsymbol{q}^s$ as

$$\boldsymbol{q}^s(x, y, t) = \int_{-\infty}^{\infty}\int_{-\infty}^{\infty} \hat{\boldsymbol{q}}^s(k_x, k_y, t) e^{i(k_x x + k_y y)}\, dk_x\, dk_y,$$

where $\hat{\boldsymbol{q}}^s = [\hat{u}_1, \hat{u}_2, \hat{v}_1, \hat{v}_2, \hat{p}_1, \hat{p}_2]^T$ represents the Fourier coefficients of the split field components. This yields the initial value problem

$$\frac{\partial \hat{\boldsymbol{q}}^s}{\partial t} = P(k_x, k_y)\hat{\boldsymbol{q}}^s, \tag{5}$$

where the symbol, $P(k_x, k_y)$, is

$$P(k_x, k_y) = -i \begin{bmatrix} 0 & 0 & 0 & 0 & k_x & k_x \\ Mk_x & Mk_x & 0 & 0 & 0 & 0 \\ 0 & 0 & 0 & 0 & k_y & k_y \\ 0 & 0 & Mk_x & Mk_x & 0 & 0 \\ k_x & k_x & 0 & 0 & Mk_x & Mk_x \\ 0 & 0 & k_y & k_y & 0 & 0 \end{bmatrix}. \tag{6}$$

Integration of Eqs. (5)–(6) is done by first realizing that the evolution of the individual split components depends only on the un-split variables. Hence, the solution for the split field variables can be derived from the solution of the Cauchy problem of Eqs. (1)–(2).

Considering the initial conditions $\hat{\boldsymbol{q}}(0) = [\hat{u}_0, \hat{v}_0, \hat{p}_0]^T$, the solution to Eqs. (1)–(2) is given on the form

$$\hat{\boldsymbol{q}}(t) = \boldsymbol{a}e^{-i(Mk_x - \nu)t} + \boldsymbol{b}e^{-i(Mk_x + \nu)t} + \boldsymbol{c}e^{-iMk_x t}, \tag{7}$$

with the three vectors $\boldsymbol{a} = [a_u, a_v, a_p]^T$, $\boldsymbol{b} = [b_u, b_v, b_p]^T$, and $\boldsymbol{c} = [c_u, c_v, c_p]^T$, having the entries

$$\boldsymbol{a} = \frac{\mu - \hat{p}_0\nu}{2\nu^2}\begin{bmatrix} k_x \\ k_y \\ -\nu \end{bmatrix}, \qquad \boldsymbol{b} = \frac{\mu + \hat{p}_0\nu}{2\nu^2}\begin{bmatrix} k_x \\ k_y \\ \nu \end{bmatrix}, \qquad \boldsymbol{c} = \frac{1}{\nu^2}\begin{bmatrix} \hat{u}_0\nu^2 - k_x\mu \\ \hat{v}_0\nu^2 - k_y\mu \\ 0 \end{bmatrix},$$

and

$$\nu = \sqrt{k_x^2 + k_y^2}, \qquad \mu = \hat{u}_0 k_x + \hat{v}_0 k_y.$$

In Eq. (7) we immediately recognize the three types of waves, inherent in the linearized Euler equations, giving rise to three different wave speeds. Moreover, we note that $\boldsymbol{a}$ and $\boldsymbol{b}$ as well as $\boldsymbol{c}$ are bounded for all values of k_x and k_y. This confirms that Eqs. (1)–(2) constitute

a strongly well-posed problem for which the solution can be bounded up to exponential growth in time by the norm of the initial data.

Integrating the solution, Eq. (7), following Eqs. (5)–(6), to obtain the solution for $\hat{\boldsymbol{q}}_2^s = [\hat{u}_2, \hat{v}_2, \hat{p}_2]^T$, we recover

$$\hat{\boldsymbol{q}}_2(t) - \hat{\boldsymbol{q}}_2(0) = \boldsymbol{a}_2^s e^{-i\frac{Mk_x-\nu}{2}t} + \boldsymbol{b}_2^s e^{-i\frac{Mk_x+\nu}{2}t} + \boldsymbol{c}_2^s e^{-i\frac{Mk_x}{2}t}, \tag{8}$$

where

$$\boldsymbol{a}_2^s = -i\frac{\sin[((Mk_x-\nu)/2)t]}{(Mk_x-\nu)/2}\begin{bmatrix} Mk_x a_u \\ Mk_x a_v \\ k_y a_v \end{bmatrix}, \qquad \boldsymbol{b}_2^s = -i\frac{\sin[((Mk_x+\nu)/2)t]}{(Mk_x+\nu)/2}\begin{bmatrix} Mk_x b_u \\ Mk_x b_v \\ k_y b_v \end{bmatrix},$$

and

$$\boldsymbol{c}_2^s = -i\frac{\sin[(Mk_x/2)t]}{Mk_x/2}\begin{bmatrix} Mk_x c_u \\ Mk_x c_v \\ k_y c_v \end{bmatrix}.$$

An equivalent result appears upon integration of $\hat{\boldsymbol{q}}_1$. For the split set of equations to be strongly well-posed we must ensure that the solution, Eq. (8), remains bounded by the norm of the initial data for any choice of k_x and k_y, or, in other words, $\boldsymbol{a}_2^s$, $\boldsymbol{b}_2^s$, and $\boldsymbol{c}_2^s$, must remain bounded for any combination of k_x and k_y. It is easily verified that $\boldsymbol{a}_2^s$ and $\boldsymbol{b}_2^s$ indeed remain bounded for all values of k_x and k_y provided the mean flow is purely subsonic, i.e., $|M| < 1$. This is only a natural constraint as reflections from the open boundary are unable to enter the computational domain in case of supersonic flow conditions.

The situation for $\boldsymbol{c}_2^s$ is very different. In the limit where $|Mk_x| \to 0$ and $|k_y| \gg |Mk_x|$ we can only bound one of the terms in $\boldsymbol{c}_2^s$ as

$$\left| k_y c_v \frac{\sin[(Mk_x/2)t]}{Mk_x/2} \right| \leq |c_v k_y| t, \tag{9}$$

i.e., we recover a term that grows in time with a coefficient, k_y, being unbounded. Hence, $\|\hat{p}_2\|$ cannot be bounded by the norm of the initial conditions, but rather depends also on the norm of the derivatives of the initial conditions. Consequently, the split set of equations, Eq. (3), is only weakly well-posed with the solution depending not only on the initial conditions but also on the smoothness of these data.

It is noteworthy that, as is the case for the split field perfectly matched layer methods of electromagnetics [10, 11], in the case where $|k_y| = 0$ strong well-posedness is recovered. Hence, the one-dimensional version of the split field method for the perfectly matched layers of acoustics is valid and well suited for numerical solution.

The loss of derivatives is as such not a severe problem. However, contrary to strongly well-posed hyperbolic problems, it is well known that weakly well-posed systems may become ill-posed under low order perturbations [19], thus rendering the systems of equations inherently unstable and proper numerical solution impossible.

To see this, we introduce a low order perturbation of the form

$$E\hat{\boldsymbol{q}}^s = \begin{bmatrix} 0 & 0 & 0 & 0 & 0 & 0 \\ 0 & 0 & 0 & 0 & 0 & 0 \\ 0 & 0 & 0 & 0 & 0 & 0 \\ 0 & 0 & \varepsilon & -\varepsilon & 0 & 0 \\ 0 & 0 & 0 & 0 & 0 & 0 \\ 0 & 0 & \varepsilon & -\varepsilon & 0 & 0 \end{bmatrix} \hat{\boldsymbol{q}}^s,$$

i.e., the perturbation corresponds to a small perturbation in the split field velocity component, $\hat{v}_1$ and $\hat{v}_2$, however maintaining that $\hat{v} = \hat{v}_1 + \hat{v}_2$. We consider the perturbed Cauchy problem

$$\frac{\partial \hat{\boldsymbol{q}}^s}{\partial t} = (P(k_x, k_y) + E)\hat{\boldsymbol{q}}^s = \tilde{P}\hat{\boldsymbol{q}}^s,$$

and recall that a necessary condition for the perturbed problem to remain well-posed is that the real parts of the eigenvalues of $\tilde{P}$ remain in the left half plane for any choice of k_x and k_y and, preferably, also for any choice of ε and M. The first 2 eigenvalues of $\tilde{P}$ are given as $\lambda_1 = \lambda_2 = 0$, while the remaining 4 eigenvalues appear as the roots of a 4th order complex polynomial.

Rather than solving the complex polynomial directly, we apply the Routh–Hurwitz criteria to arrive at conditions under which the perturbed initial value problem remains well-posed. This procedure yields, as a necessary condition for well-posedness, that

$$|Mk_x| > |k_y|.$$

which is very similar to the limit for boundedness of $\boldsymbol{c}_2^s$, Eq. (9), and confirms that the weakly well-posed system, arrived at by splitting the linearized Euler equations in order to develop the perfectly matched layers, becomes ill-posed under low order perturbations. We should note that there is nothing particular about the low order perturbation, E, i.e., ill-posedness can be shown for perturbations of the velocity components as well as of the pressure.

In an actual numerical implementation of the split field equations the sensitivity to perturbations, which are bound to happen due to finite precision, can be expected to result in severe problems with maintaining stability of the scheme. This is indeed exactly what was reported in [17, 18] where it was found that applying a filter in the PML layers was necessary to maintain stability. An indication of why the filter has a stabilizing effect for this problem is provided by the condition for boundedness, Eq. (9). If the filter is sufficiently strong as to ensure that $|Mk_x| > |k_y|$ for all values of $|k_x|$ and $|k_y|$, e.g., by applying a strong filter along y, the system remains well-posed and, as a consequence, the scheme might recover stability or at least postpone the effects of the instability.

4. THE CONSTRUCTION OF WELL-POSED PML METHODS

The weakly well-posedness and associated ill-posedness under small perturbations of the split-field PML equations were recently shown [11] also for the original PML method as proposed in [10] and several strongly well-posed PML methods for the equations of electromagnetics have recently been proposed, see, e.g., [12–16] and references therein. Hence, rather than attempting an ab initio development of perfectly absorbing layers for the

linearized Euler equations, we shall utilize the recent developments to arrive at the sought after well behaved methods.

A strongly well-posed PML method for the Maxwells equations is proposed in [16] and tested numerically in [15] and we shall base the remaining part of this paper on this particular formulation. We should emphasize though that alternative well-posed formulations might equally well be employed as the basis of the development of the PML methods for the equations of acoustics.

4.1. The Non-Convecting Case

Let us first consider the simple case of a non-convecting free-stream, i.e., $M = 0$ in Eqs. (1)–(2). We propose to consider an absorbing layer for the non-convecting linearized Euler equations of the form [16]

$$\begin{aligned}
\frac{\partial \rho}{\partial t} &= -\frac{\partial u}{\partial x} - \frac{\partial v}{\partial y} - \varepsilon' Q_x - \mu' Q_y, \\
\frac{\partial u}{\partial t} &= -\frac{\partial p}{\partial x} - 2\varepsilon u - \varepsilon P_x, \\
\frac{\partial v}{\partial t} &= -\frac{\partial p}{\partial y} - 2\mu v - \mu P_y, \\
\frac{\partial p}{\partial t} &= -\frac{\partial u}{\partial x} - \frac{\partial v}{\partial y} - \varepsilon' Q_x - \mu' Q_y, \\
\frac{\partial P_x}{\partial t} &= \varepsilon u, \qquad \frac{\partial Q_x}{\partial t} = -\varepsilon Q_x + u, \\
\frac{\partial P_y}{\partial t} &= \mu v, \qquad \frac{\partial Q_y}{\partial t} = -\mu Q_y + v.
\end{aligned} \tag{10}$$

Here, $\varepsilon = \varepsilon(x)$ and $\mu = \mu(y)$ signifies the non-dimensional damping parameters. We immediately note that since the Euler equations are altered by low-order terms only, the system of partial differential equations is well-posed by construction while the additional freedom, required for obtaining the sought after properties of the matched layers, is introduced through 4 additional equations describing the development of the artificial fields, P_x and Q_x, along x and, likewise, P_y and Q_y, along y. In general, we assume that the absorbing region is outside a square bounded by $|x| = a$ and $|y| = b$ while the specification of the parameters, ε and μ remains open at this point in time.

To come to an understanding of the properties of this absorbing layer we follow the analysis introduced in [11, 16] and study the behavior of a plane wave hitting the layer interface, which we assume is positioned at $x = 0$. As the system is purely linear, it poses no restrictions only to consider the behavior of plane waves as any type of excitation can be decomposed into a superposition of such plane waves of the form

$$\begin{bmatrix} u \\ v \\ p \end{bmatrix} = \begin{bmatrix} \alpha \\ \beta \\ 1 \end{bmatrix} e^{i\omega(t-\alpha x-\beta y)}, \tag{11}$$

where $\alpha^2 + \beta^2 = 1$ represents the arbitrary angle of incidence and ω signifies the normalized frequency of the incoming wave.

We shall seek solutions inside a layer in the x-direction, i.e., $\mu(y) = 0$ in Eq. (10), of the form

$$\begin{bmatrix} u \\ v \\ p \\ Q_x \\ P_x \end{bmatrix} = \begin{bmatrix} \tilde{u}(x) \\ \tilde{v}(x) \\ \tilde{p}(x) \\ \tilde{Q}_x(x) \\ \tilde{P}_x(x) \end{bmatrix} e^{i\omega(t-\beta y)}. \tag{12}$$

Introducing Eq. (12) into Eq. (10) yields the equations

$$\tilde{v} = \beta\tilde{p}, \qquad \tilde{Q}_x = \frac{1}{\psi}\tilde{u}, \qquad \tilde{P}_x = \frac{\varepsilon}{i\omega}\tilde{u}, \tag{13}$$

expressing 3 of the 5 variables in terms of $\tilde{u}$ and $\tilde{p}$, which are governed by the coupled equations

$$\frac{d}{dx}\tilde{p} = -\frac{\psi^2}{i\omega}\tilde{u}, \qquad \frac{d}{dx}[\psi\tilde{u}] = -i\omega\psi\alpha^2\tilde{p},$$

where we have introduced $\psi(x) = i\omega + \varepsilon(x)$. Combining these two equations yields a second order variable coefficient ODE for $\tilde{p}$ on the form

$$\frac{d}{dx}\left(\frac{1}{\psi}\frac{d}{dx}\tilde{p}\right) = \psi\alpha^2\tilde{p},$$

with the analytical solution

$$\tilde{p}(x) = Ae^{\alpha\int_0^x \psi(\eta)\,d\eta} + Be^{-\alpha\int_0^x \psi(\eta)\,d\eta}, \tag{14}$$

through which the solution to $\tilde{u}$ appears as

$$\tilde{u}(x) = -\frac{i\omega}{\psi^2}\frac{d}{dx}\tilde{p}(x) = -\alpha\frac{i\omega}{\psi}\left(Ae^{\alpha\int_0^x \psi(\eta)\,d\eta} - Be^{-\alpha\int_0^x \psi(\eta)\,d\eta}\right). \tag{15}$$

The remaining fields are then given from this using Eq. (13).

The specification of A and B naturally depends on the boundary conditions we choose to impose and there are indeed several ways of doing so. We shall assume that the layer has a finite width, d, and shall hence need to impose boundary conditions at $x = 0$ and $x = d$. For the solution of hyperbolic systems it is most natural to impose characteristic boundary conditions by specifying the incoming characteristics. This amounts to requiring that $p + u$ remains continuous across the interface $x = 0$ while $p - u = 0$ at $x = d$, i.e., no information enters the layer. Imposing these boundary conditions, using Eq. (11), implies

$$\tilde{p}(0) + \tilde{u}(0) = 1 + \alpha, \qquad \tilde{p}(d) - \tilde{u}(d) = 0,$$

from which we arrive at ($\alpha \neq 0$)

$$A = \frac{\alpha - \gamma}{\alpha + \gamma}e^{-2\alpha I}B, \qquad B = \frac{1}{1 + \frac{\alpha-\gamma}{\alpha+\gamma}\frac{1-\alpha}{1+\alpha}e^{-2\alpha I}}, \tag{16}$$

where

$$\gamma = \frac{\varepsilon(d) + i\omega}{i\omega}, \qquad I = \int_0^d \psi(\eta)\, d\eta = i\omega d + \int_0^d \varepsilon(\eta)\, d\eta.$$

Combining Eq. (13) with Eqs. (14)–(16) yields the complete solution inside the layer on the form

$$\begin{aligned}
u(x,y,t) &= -B\alpha \frac{i\omega}{\varepsilon(x)+i\omega}\left[1 - \frac{\alpha-\gamma}{\alpha+\gamma} e^{2i\omega\alpha(x-d)} e^{-2\alpha\int_x^d \varepsilon(\eta)\,d\eta}\right] \\
&\quad \times e^{i\omega(t-\alpha x-\beta y)} e^{-\alpha\int_0^x \varepsilon(\eta)\,d\eta}, \\
v(x,y,t) &= \beta B\left[1 + \frac{\alpha-\gamma}{\alpha+\gamma} e^{2i\omega\alpha(x-d)} e^{-2\alpha\int_x^d \varepsilon(\eta)\,d\eta}\right] e^{i\omega(t-\alpha x-\beta y)} e^{-\alpha\int_0^x \varepsilon(\eta)\,d\eta}, \\
p(x,y,t) &= B\left[1 + \frac{\alpha-\gamma}{\alpha+\gamma} e^{2i\omega\alpha(x-d)} e^{-2\alpha\int_x^d \varepsilon(\eta)\,d\eta}\right] e^{i\omega(t-\alpha x-\beta y)} e^{-\alpha\int_0^x \varepsilon(\eta)\,d\eta}, \\
P_x(x,y,t) &= -B\alpha \frac{\varepsilon(x)}{\varepsilon(x)+i\omega}\left[1 - \frac{\alpha-\gamma}{\alpha+\gamma} e^{2i\omega\alpha(x-d)} e^{-2\alpha\int_x^d \varepsilon(\eta)\,d\eta}\right] \\
&\quad \times e^{i\omega(t-\alpha x-\beta y)} e^{-\alpha\int_0^x \varepsilon(\eta)\,d\eta}, \\
Q_x(x,y,t) &= B\alpha \frac{i\omega}{(\varepsilon(x)+i\omega)^2}\left[1 - \frac{\alpha-\gamma}{\alpha+\gamma} e^{2i\omega\alpha(x-d)} e^{-2\alpha\int_x^d \varepsilon(\eta)\,d\eta}\right] \\
&\quad \times e^{i\omega(t-\alpha x-\beta y)} e^{-\alpha\int_0^x \varepsilon(\eta)\,d\eta}.
\end{aligned} \tag{17}$$

Since $|\frac{i\omega}{\varepsilon+i\omega}| < 1$ all components in the layer are bounded by $|p|$ which is bounded like $\alpha\frac{\partial|p|}{\partial x} \le 0$ with equality only for grazing waves, i.e., for $\alpha = 0$. Thus, all waves are damped independent of frequency and angle of incidence as should be required by a truly perfectly matched layer.

We observe that the fields at the layer interface, $x = 0$, in general are discontinuous with a jump proportional

$$\frac{1 \pm \frac{\alpha-\gamma}{\alpha+\gamma} e^{-2i\omega\alpha d} e^{-2\alpha I}}{1 + \frac{\alpha-\gamma}{\alpha+\gamma}\frac{1-\alpha}{1+\alpha} e^{-2\alpha I}},$$

which, however, is exponentially small.

Naturally, an analysis equivalent to the above can be completed for a PML layer in the y-direction while a corner region, in which $\varepsilon > 0$ as well as $\mu > 0$, can be analyzed using separation of variables, yielding results similar to the above.

4.1.1. *A Numerical Example*

In order to confirm the theoretical analysis put forward in the previous section and study the efficiency of this new PML method, we have implemented the scheme on an equidistant grid using a 4th order centered finite-difference scheme with 3rd order closure for stability in space, while we use a 4th order Runge–Kutta scheme for advancing the equations in time. The time step, Δt, is chosen to be well below the stability limit. Contrary to the scheme proposed in [17], there is no need for applying a filter to maintain stability and, to emphasize this point, we have not used any filters in the present work.

The initial conditions are taken from benchmark problems of computational aeroacoustic [21]

$$\begin{aligned}
\rho(x,y) &= e^{-(\ln 2)\frac{(x-x_a)^2+(y-y_a)^2}{\delta_a^2}} + 0.1e^{-(\ln 2)\frac{(x-x_b)^2+(y-y_b)^2}{\delta_b^2}},\\
u(x,y) &= 0.05(y-y_b)e^{-(\ln 2)\frac{(x-x_b)^2+(y-y_b)^2}{\delta_b^2}},\\
v(x,y) &= -0.05(x-x_b)e^{-(\ln 2)\frac{(x-x_b)^2+(y-y_b)^2}{\delta_b^2}},\\
p(x,y) &= e^{-(\ln 2)\frac{(x-x_a)^2+(y-y_a)^2}{\delta_a^2}},
\end{aligned} \tag{18}$$

where (x_a, y_a) signifies the center of the initial sound pulse of width δ_a, while (x_b, y_b) refers to the center of the initial vorticity and entropy pulse of width δ_b.

The profiles, $\varepsilon(x)$ and $\mu(y)$, required in Eq. (10), are chosen as

$$\varepsilon(x) = C_x\left(\frac{|x-a|}{x_{PML}}\right)^n, \qquad \mu(y) = C_y\left(\frac{|y-b|}{y_{PML}}\right)^n. \tag{19}$$

Here we assume that the computational domain is bounded by $|x| \le a$ and $|y| \le b$ while x_{PML} and y_{PML} refers to the width of the absorbing layers along x and y, respectively. The constants, C_x, C_y, and n, control the strength of the layer and we have chosen these parameters as $C_x = C_y = 2$ and $n = 3$. The auxiliary equations of Eq. (10) are advanced in time using the same scheme and time-step as for the Euler equations themselves.

We consider the problem in the computational domain $(x, y) \in [-50, 50]^2$ with the absorbing layers outside and position the acoustics pulse at $(x_a, y_a) = (-25, 0)$ with a width of $\delta_a = 3$ while the non-propagating vorticity/entropy pulse is positioned at $(x_b, y_b) = (25, 0)$ with a width of $\delta_b = 4$. The absorbing layers are terminated using characteristic boundary conditions as discussed during the analysis of the scheme.

In Fig. 1 we show the pressure field at various times as computed using $\Delta x = \Delta y = 1$ and $\Delta t = 1$ and $x_{PML} = y_{PML} = 10$, i.e., 10 computational cells in the absorbing layer.

As expected from the analysis, the sound wave propagates undisturbed out of the computational domain with no visible reflections. The high frequency noise visible on the contours is a consequence of the accuracy of the scheme and the lack of filtering rather than a result of reflections as can also be observed on Fig. 2, where we show the u-velocity field propagating undisturbed out of the computational domain.

To verify the dependency of the efficiency of the absorbing layer on the width of the layer, we have computed the maximum pressure error along the line $x = -48$ as a function of time. In Fig. 3 we show the development of the pressure error for various layer widths as compared with using only characteristic boundary conditions to terminate the computational domain.

Indeed, as expected we see that even for a layer of only 6 cells does the PML scheme out-perform the characteristic BC in terms of accuracy while increasing the width of the layer yields a significant increase in accuracy.

As compared to the scheme in [17] we observe a slight increase in the maximum error, which is consistent with the observations made in [15] when comparing the split and un-split PML methods for Maxwells equations. A direct comparison, however, is difficult due to differences in the computational scheme and boundary conditions. We emphasize, though, that the present results are arrived at without the use of filtering, thus confirming the stability

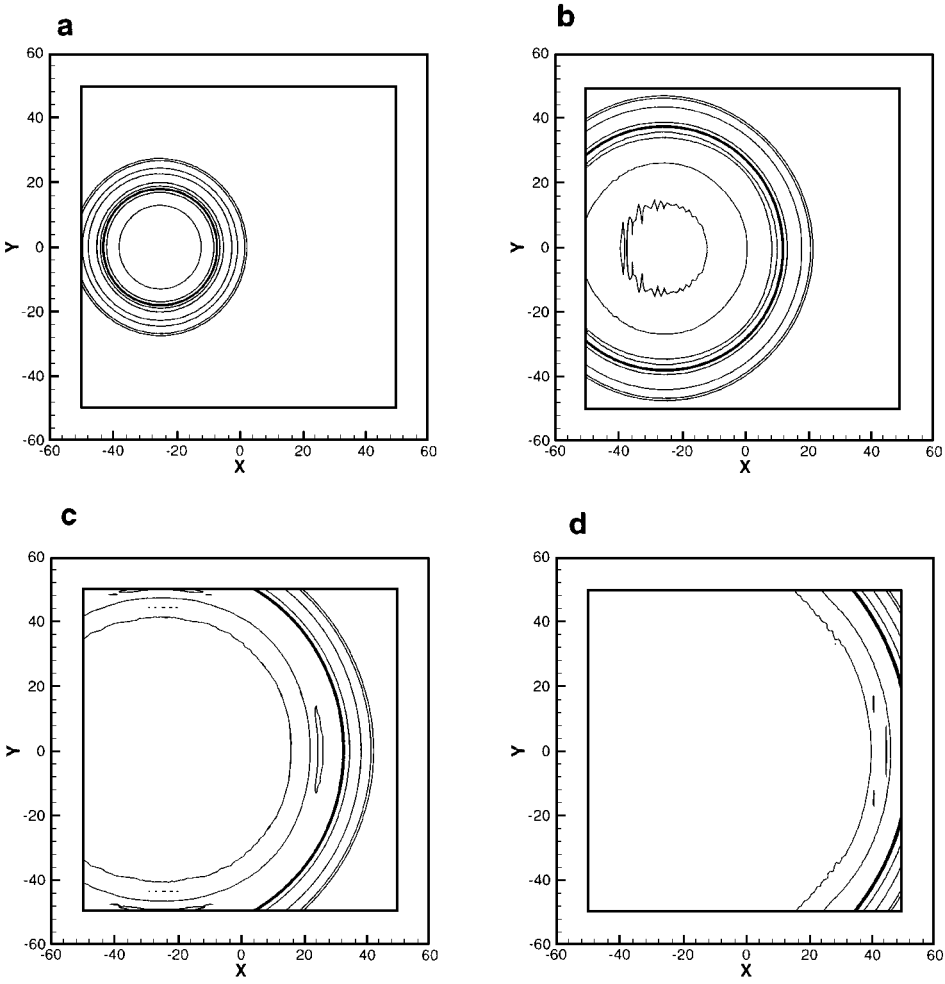

FIG. 1. Pressure contours for a sound pulse, propagating in a non-convecting medium. The contour levels are ± 0.1, ± 0.05, ± 0.01, and ± 0.005 with the computed result given at (a) $t = 20$, (b) $t = 40$, (c) $t = 60$, and (d) $t = 80$.

of the scheme given in Eq. (10) and the associated analysis of well-posedness and decaying properties of the fields inside the layers.

4.2. The Convecting Case

While the development of PML methods for the non-convecting equations of acoustics relies on the analogy with the equations of electromagnetics, no such connection is possible in the more general case of a convecting mean flow.

The first idea that comes to mind is to introduce a new reference frame, moving with a speed of M along x and then apply the PML scheme developed in Subsection 4.1. This approach, however, has the unfortunate consequence that the layer interface becomes a moving interface in physical space. In [22] the use of a transformation, connecting the convecting and non-convecting wave-equations, is suggested in order to transform the non-convecting PML method such as to be useful in the convecting case. While this approach

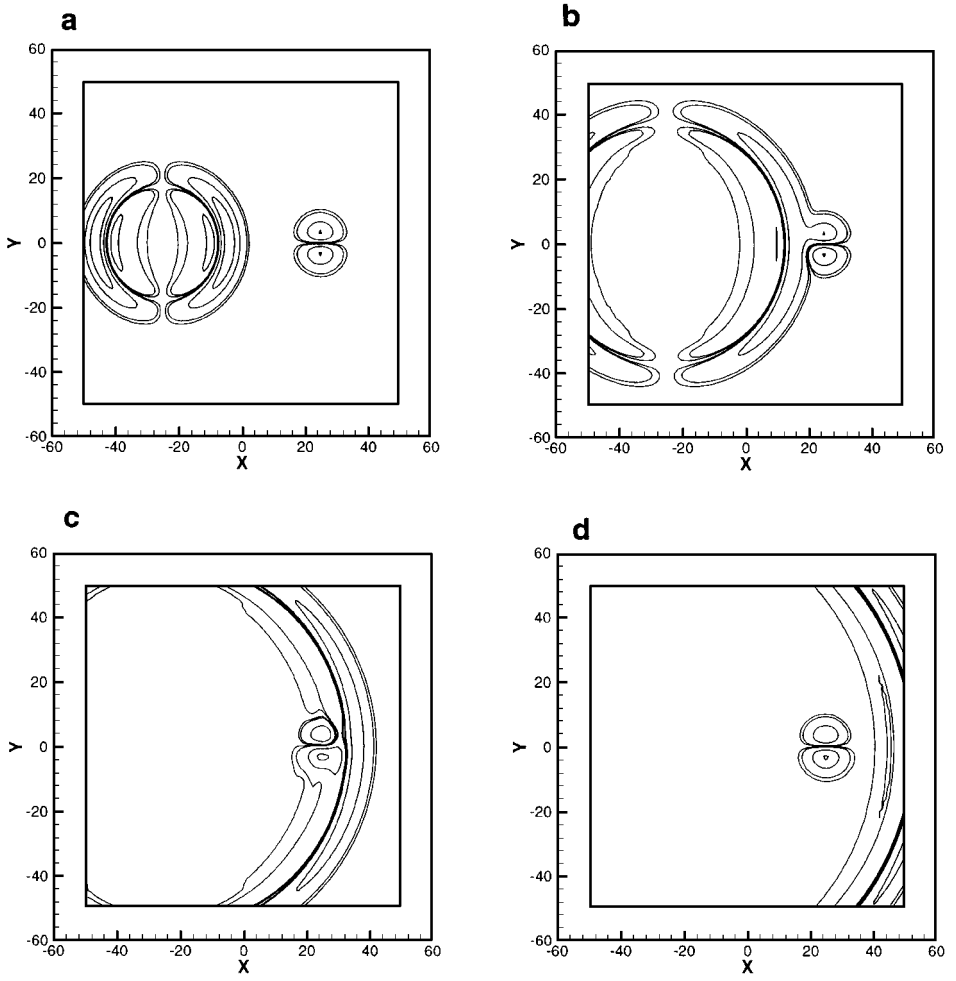

FIG. 2. u-velocity contours for a sound pulse, propagating in a non-convecting medium. The contour levels are ± 0.1, ± 0.05, ± 0.01, and ± 0.005 with the computed result given at (a) $t = 20$, (b) $t = 40$, (c) $t = 60$, and (d) $t = 80$.

turns out to work well for the sound-waves, the resulting PML method has an abruptly changing convective velocity for the entropy and vorticity waves, resulting in significant reflections from such waves which become non-convecting exactly at the layer-interface. Moreover, the correct use of this approach in the corner regions of the PML layers is much less clear.

Here we shall take a different approach although we shall rely on the PML schemes developed in the previous section combined with a few other techniques. Introducing layers in which the flow is accelerated into a supersonic region, thereby eliminating the need for absorbing boundary conditions, was recently proposed in [7] and modified in [9]. While this approach is appealing, it has an undesirable effect on the time-step of the whole computation and primitive sponge layers are still needed to yield an acceptable performance [9].

We propose to decelerate the flow, rather than accelerating it, towards a non-convecting flow inside the layer and then combine this approach with the PML scheme developed in Subsection 4.1. While such a scheme cannot be expected to be perfectly absorbing in the

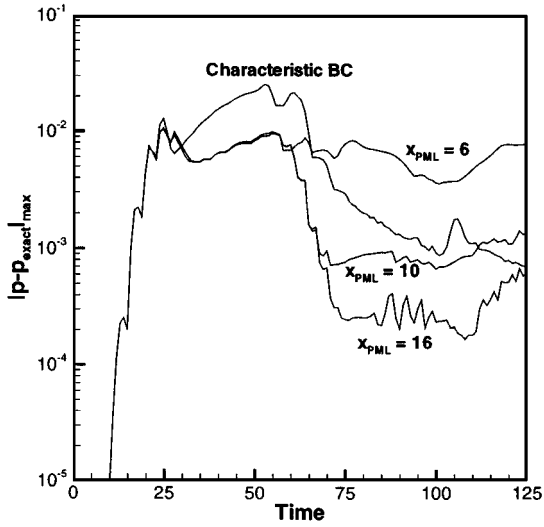

FIG. 3. Maximum error at $x = -48$ as a function of time as computed with different types of boundary conditions and varying width of the PML layer.

case of a finite layer, it does have the potential of a very efficient absorption, provided the deceleration is done appropriately and that the layer width is chosen accordingly.

We propose to consider a PML-like scheme for the convecting case, Eqs. (1)–(2), of the form

$$\begin{aligned}
\frac{\partial \rho}{\partial t} + M[1-m(x)]\frac{\partial \rho}{\partial x} &= -\frac{\partial u}{\partial x} - \frac{\partial v}{\partial y} - \varepsilon' Q_x - \mu' Q_y - \sigma M \rho,\\
\frac{\partial u}{\partial t} + M[1-m(x)]\frac{\partial u}{\partial x} &= -\frac{\partial p}{\partial x} - 2\varepsilon u - \varepsilon P_x,\\
\frac{\partial v}{\partial t} + M[1-m(x)]\frac{\partial v}{\partial x} &= -\frac{\partial p}{\partial y} - 2\mu v - \mu P_y - \sigma M v,\\
\frac{\partial p}{\partial t} + M[1-m(x)]\frac{\partial p}{\partial x} &= -\frac{\partial u}{\partial x} - \frac{\partial v}{\partial y} - \varepsilon' Q_x - \mu' Q_y,\\
\frac{\partial P_x}{\partial t} &= \varepsilon u, \qquad \frac{\partial Q_x}{\partial t} = -\varepsilon Q_x + u,\\
\frac{\partial P_y}{\partial t} &= \mu v, \qquad \frac{\partial Q_y}{\partial t} = -\mu Q_y + v.
\end{aligned} \tag{20}$$

Here ε and μ remain unchanged from Subsection 4.1 and we have introduced $m(x)$, which provides the decelerating term by being $m(a) \simeq 0$, with $x = a$ signifying the layer interface, while we require that $m(a + x_{PML}) \simeq 1$ at the termination of the absorbing layer. We have found that using the error function provides a good compromise between steepness and smoothness such that

$$m(z) = \frac{1}{2}\left[1 + \frac{2}{\sqrt{\pi}}\int_0^{\sigma_m[z-x_m]} e^{-t^2} dt\right], \tag{21}$$

where $z = (x - a)/x_{PML}$ and σ_m and x_m control the steepness and relative position of the profile, respectively. In Eq. (20) we have also introduced simple absorbing terms in

the equations for ρ and v. Since the non-convecting PML scheme only is perfectly absorping for the sound waves, this is meant to provide a simple mechanism for damping of the entropy and vorticity waves inside the layer. The parameters $\sigma(x)$ can be used to control the strength of this sponge layer for ρ and v.

A few comments regarding the scheme, Eq. (20), are in place. First of all we note that for $M = 0$ we recover Eq. (10). Also since only the diagonal entries of A in Eqs. (1)–(2) are altered the well-posedness of the equations of acoustics remains intact. The philosophy here is that as the convective waves are slowed down, they approach the case of the non-convecting acoustics for which Eq. (10) was shown to perform well. Moreover, slowly decelerating the waves as they enter the layer has the additional advantage that the wave fronts become increasingly normal to the boundary of the layer—much like the water wave always being aligned with the beach. Hence, applying characteristic boundary conditions for truncating the PML layer can be expected to be efficient.

4.2.1. *A Numerical Example*

In order to establish the soundness of the arguments that lead to the PML-like scheme in Eq. (20), we have conducted a number of experiments using the scheme and the initial conditions described in Subsection 4.1.1 with $M = 0.5$ as the convective Mach number of the mean flow.

The decelerating term, Eq. (21), is generally specified by using $\sigma_m = 5$ and $x_m = 0.5$, i.e., the profile is centered in the middle of the absorbing layer. We have taken $\sigma(x) = \varepsilon(x)$, although this is by no means a unique choice and alternatives might well yield better performance than reported here.

Since the layer now has multiple functions, i.e., it decelerates the waves while also acting as an absorbing layer, it is expected that, compared to the non-convecting case, slightly wider layers should be used to achieve an acceptable accuracy.

In Fig. 4 we show the temporal development of the density for the initial conditions given in Eq. (18) with ε and μ being given in Eq. (19) and the parameters chosen as in Subsection 4.1.1. We have taken the width of the layer as $x_{PML} = y_{PML} = 20$, i.e., 20 computational cells, and $\Delta t = 0.5$. The exact solution is given in [21].

As expected, the sound pulse as well as the entropy pulse leaves the computational domain with no noticeable reflections from the layer. In Fig. 5 we show the development of the u-velocity component, arriving at similar conclusions.

To address, in a more quantitative manner, the accuracy of the proposed scheme as a function of the width of the layer we compute the maximum error in the pressure along the line $x = 48$ as a function of time. In Fig. 6 we plot the results for increasing the width of the layer and compare them to the accuracy obtained when using only a characteristic boundary condition to terminate the computational domain.

Indeed we find that using a layer of only 10 cells yields an overall accuracy of the order of the approximation error of the scheme and is superior to that obtained using characteristic boundary conditions only. By increasing the width of the layer 20 cells we observe a significant reduction, much like the case of the true PML in Fig. 3, of the reflections from the layer.

As expected, a slightly wider layer, as compared to the results in Subsection 4.1.1, is required in order to obtain an acceptable accuracy. However, rather than increasing the number of cells in the layer one could use a mapping, thereby stretching the grid, combined

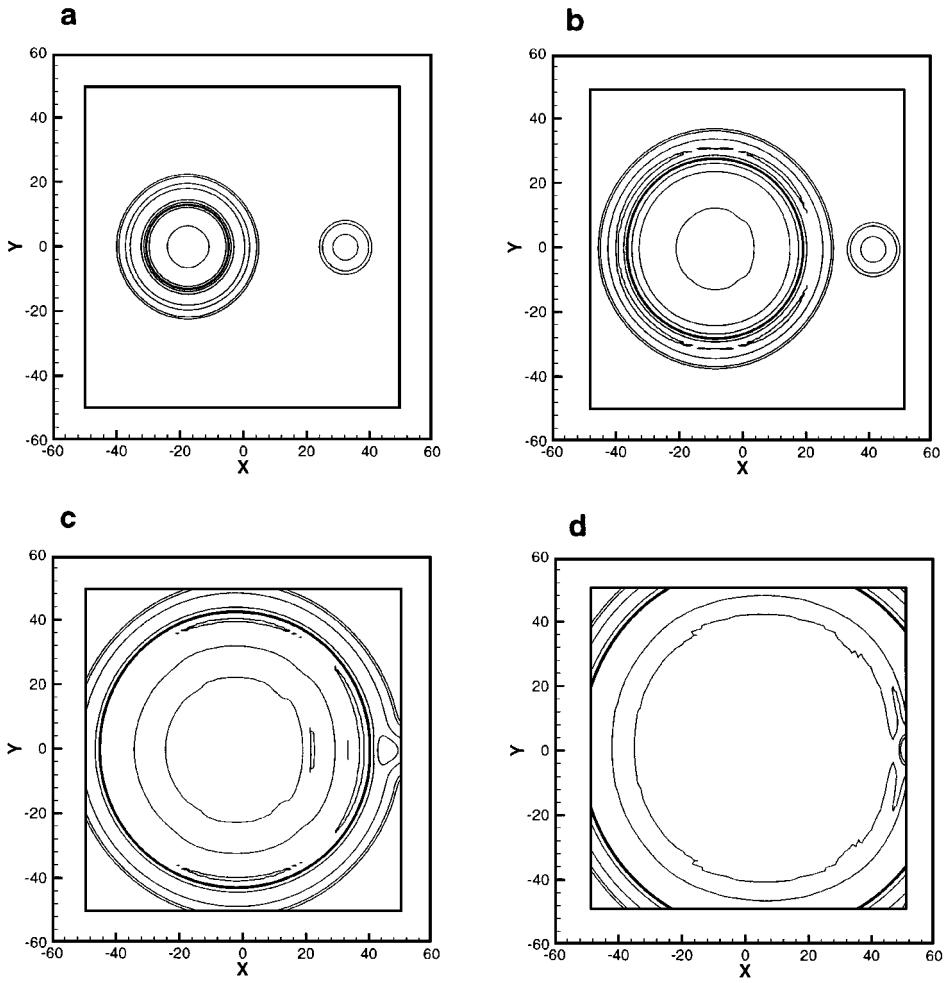

FIG. 4. Density contours for a sound and entropy pulse, propagating in a convecting medium with $M = 0.5$. The contour levels are ± 0.1, ± 0.05, ± 0.01, and ± 0.005 with the computed result given at (a) $t = 15$, (b) $t = 30$, (c) $t = 45$, and (d) $t = 60$.

with a filter inside the layer. This approach was proposed in [6] for the case of acoustics and successfully used for the case of electromagnetics in [14, 15]. While this approach certainly will improve on the performance of the scheme with only a little extra computational effort, we have chosen not to implement this technique in order to emphasize that the present schemes do not require the use of a filter in order to maintain stability.

5. CONCLUDING REMARKS

The purpose of this paper has been twofold. In the first part of the paper we provide an analysis of a recently proposed PML method for the equations of acoustics [17]. As remarked in [17, 18] these PML methods suffer from intrinsic numerical instabilities and we gave an explanation for this in terms of loss of well-posedness of the split set of equations and, as a result of this, the appearance of ill-posedness under small arbitrary perturbations. Such perturbations will inevitably exist in any numerical implementation of the split set of

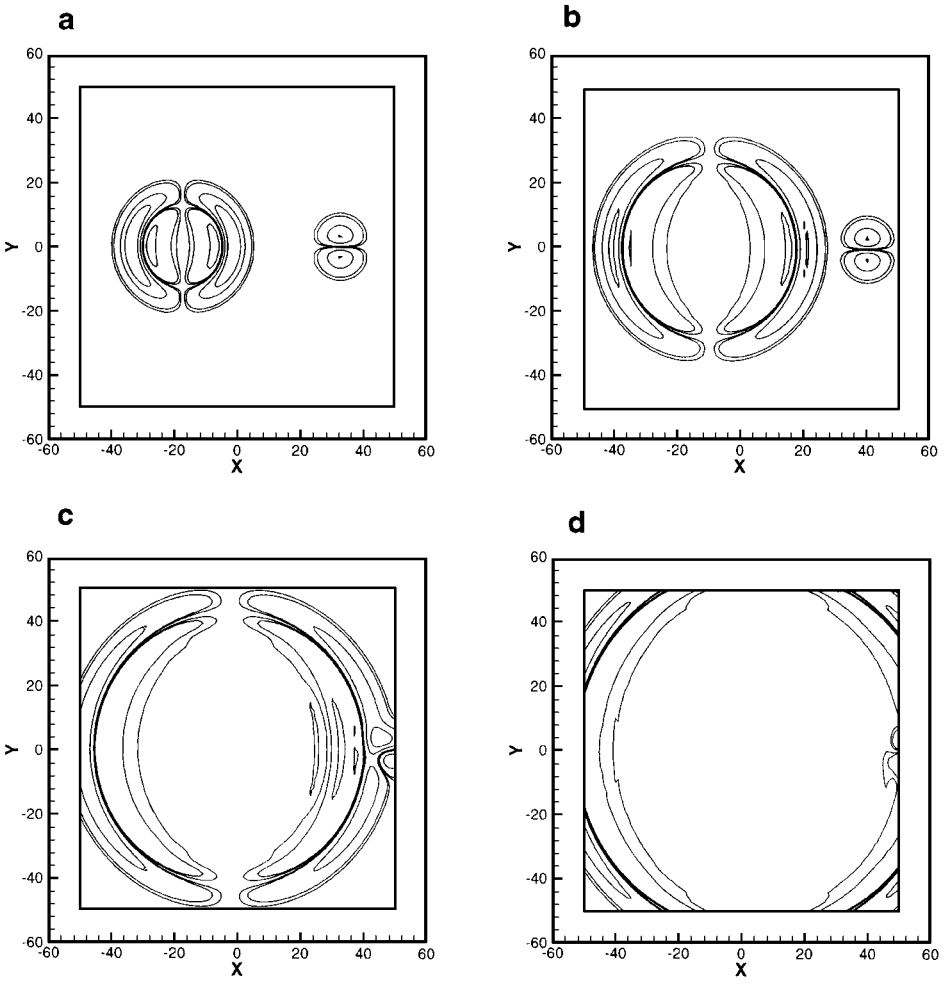

FIG. 5. u-velocity contours for a sound and vorticity pulse, propagating in a convecting medium with $M = 0.5$. The contour levels are ± 0.1, ± 0.05, ± 0.01, and ± 0.005 with the computed result given at (a) $t = 15$, (b) $t = 30$, (c) $t = 45$, and (d) $t = 60$.

equations, rendering the schemes inherently unstable unless some kind of high-frequency damping, e.g., in the form of a low-pass filter, is introduced.

The use of filters is a subject of some controversy. We believe, however, that while there might be numerous physical arguments for applying filters in various situations, it is a concern if the numerical scheme, rather than the physics, dictates the need for a filter as is the case of the PML methods in [17]. Indeed, in situations where smooth initial conditions and only smooth boundaries are considered it is troublesome if the solution of a linear hyperbolic system requires the use of filters.

In the second part of the paper we present a PML scheme for the non-convective equations of acoustics and prove that it is indeed absorbing for all frequencies and angle of incidence while maintaining strong well-posedness. The properties of the layer are studied in more detail through numerical tests, confirming the analysis.

In the general case of a convecting mean flow, the approach taken here is less rigorous. While we present an absorbing layer scheme that exhibits PML-like behavior, it is strictly

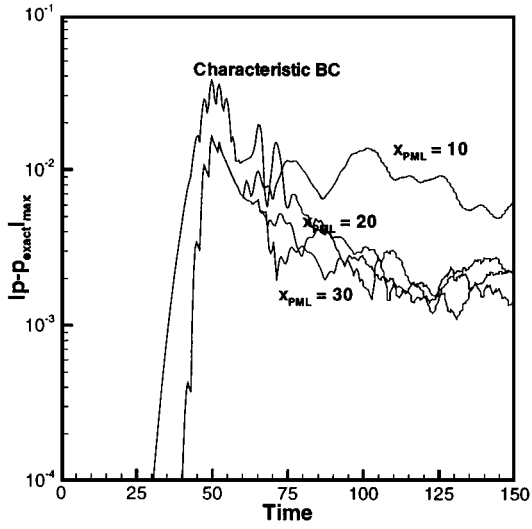

FIG. 6. Maximum error at $x = 48$ as a function of time as computed with different types of boundary conditions and varying depth of the absorbing layer.

speaking not a PML method but rather a scheme arrived at by combining several techniques. The scheme remains well-posed and performs well, although it requires the use of a slightly wider layer as compared to the true PML method presented earlier. The advantage of this scheme is that it contains the true PML scheme in the limit of a vanishing mean velocity and extends trivially to the general case of a mean flow which is not aligned with the axis.

The development of a true well-posed PML method for the convective equations of acoustics remains an open challenge due the complication introduced by the appearance of several types of waves and a preferred direction of propagation. We hope to address these important issues in a future paper.

ACKNOWLEDGMENTS

The author expresses his gratitude to Professor D. Gottlieb, Brown University, for inspiring and enlightening conversations. This work was supported by DOE Grant DE-FG02-95ER25239 and NSF Grant ASC-9504002.

REFERENCES

1. K. W. Thompson, Time dependent boundary conditions for hyperbolic systems, *J. Comput. Phys.* **68**, 1 (1987).
2. B. Engquist and A. Majda, Absorbing boundary conditions for the numerical simulation of waves, *Math. Comp.* **31**, 629 (1977).
3. R. L. Higdon, Numerical absorbing boundary conditions for the wave equation, *Math. Comp.* **49**, 65 (1987).
4. A. Bayliss and E. Turkel, Radiation boundary conditions for wave-like equations, *Comm. Pure Appl. Math.* **33**, 707 (1980).
5. D. Givoli, Non-reflecting boundary conditions, *J. Comput. Phys.* **94**, 1 (1991).
6. T. Colonius, S. K. Lele, and P. Moin, Boundary conditions for direct computation of aerodynamic sound generation, *AIAA J.* **31**, 1574 (1993).
7. S. Ta'asan and D. M. Nark, "An Absorbing Buffer Zone Technique for Acoustic Wave Propagation," AIAA Paper 95-0146, 1995.

8. K. Mazaheri and P. L. Roe, Numerical wave propagation and steady-state solutions: Soft wall and outer boundary conditions, *AIAA J.* **35**, 965 (1997).
9. J. B. Freund, Proposed inflow/outflow boundary conditions for direct computation of aerodynamic sound, *AIAA J.* **35**, 740 (1997).
10. J.-P. Berenger, A perfectly matched layer for the absorption of electromagnetic waves, *J. Comput. Phys.* **114**, 185 (1994).
11. S. Abarbanel and D. Gottlieb, A mathematical analysis of the PML method, *J. Comput. Phys.* **134**, 357 (1997).
12. L. Zhao and A. C. Cangellaris, A general approach for the development of unsplit-field time-domain implementations of perfectly matched layers for FD-TD grid truncation, *IEEE Microwave Guided Wave Lett.* **6**, 209 (1996).
13. R. W. Ziolkowski, Time-derivative Lorentz-material model based absorbing boundary conditions, *IEEE Trans. Antennas Propagat.* **45**, 656 (1997).
14. B. Yang, D. Gottlieb, and J. S. Hesthaven, Spectral simulations of electromagnetic wave scattering, *J. Comput. Phys.* **134**, 216 (1997).
15. B. Yang, D. Gottlieb, and J. S. Hesthaven, On the use of PML ABC's in spectral time-domain simulations of electromagnetic scattering, in *Proc. of ACES 13'th Annual Review of Progress in Applied Computational Electromagnetics, Monterey, 1997*, pp. 926–933.
16. S. Abarbanel and D. Gottlieb, On the construction and analysis of absorbing layers in CEM, in *Proc. of ACES 13'th Annual Review of Progress in Applied Computational Electromagnetics, Monterey, 1997*, pp. 876–883.
17. F. Q. Hu, On absorbing boundary conditions for linearized Euler equations by a perfectly matched layer, *J. Comput. Phys.* **129**, 201 (1996).
18. J. W. Goodrich and T. Hagstrom, "A Comparison of Two Accurate Boundary Treatments for Computational Aeroacoustics," AIAA Paper 97-1585, 1997.
19. B. Gustavsson, H. O. Kreiss, and J. Oliger, "*Time Dependent Problems and Difference Methods*" (Wiley, New York, 1995).
20. S. Abarbanel and D. Gottlieb, Optimal time splitting methods for the Navier–Stokes equations and two- and three space variables, *J. Comput. Phys.* **41**, 1 (1981).
21. J. C. Hardin, J. R. Ristorcelli, and C. K. W. Tam (Eds.), *ICASE/LaRC Workshop on Benchmark Problems in Computational Aeroacoustics (CAA)* NASA CP 3300, NASA Langley Research Center, 1995).
22. E. Turkel and A. Yefet, Absorbing PML boundary layers for wave-like equations, *Appl. Numer. Math.*, in press.